

D⁰ reconstruction for CDR

10k Hijing Au+Au 200 GeV central events are produced in full STAR geometry environment with new updates. The new beam pipe is designed with a radius of 2 cm from the detector center and a thickness of 0.0762 cm. The pile-up effect was included in the PIXEL simulation at a rate corresponding to RHIC-II luminosity. The event vertex resolution is 0.01 cm in X-Y and 20 cm in Z assuming Gaussian distributions. Events are only generated within ± 5 cm in V_z from detector center. 5 D⁰s were embedded flat in p_T (0.2-10 GeV/c) or following power-law distribution (0.2-5 GeV/c) in each Hijing central event with 100% branching ratio (B.R.) decay to hadronic channel ($D^0 \rightarrow K^- \pi^+$, B.R. |_{PDG} = 3.83%). The pseudo-rapidity distribution is flat in ± 1 and azimuthal angle distribution is flat in 2π . Their daughter particles K, π were identified via selection on the m^2 distribution provided by the full barrel Time-of-Flight detector (BTOF) with 100ps timing resolution.

The D⁰ was reconstructed with the same topological cuts as those in CD0. The additional TOF m^2 cuts were applied at low p_T (<3 GeV/c) for $K\pi$ identification. Tracks with large m^2 were rejected as protons. At high p_T (>3 GeV/c), $K\pi$ can not be separated, only m^2 cut applied for proton rejection. Mis-identification of $K\pi$ is included in the background estimation.

The D⁰ reconstruction efficiencies in Au+Au 200 GeV central collisions are shown in Figure 1. Squares and circles are D⁰ efficiencies before and after applying the topological cuts, respectively. The D0 efficiency in CD0 is shown as black solid symbols. In order to have good statistics at high p_T , the embedded D0 p_T was input as a flat distribution. The efficiency with thin PXL geometry was shown as red open symbols, while the one with thick PXL geometry was shown as blue open symbols. At low p_T (<3.5 GeV/c), a power-law distribution with $\langle p_T \rangle = 1$ GeV/c, $n = 11$ was used as the input D0 p_T distribution to reduce the statistics error of the efficiencies, one of which with thin PXL geometry was shown as red solid symbols, while the other with thick PXL geometry was shown as blue solid symbols.

The “thin” and “thick” geometries are corresponding to the mass of the IST and PIXEL (PXL) layers.

Thin PXL $\sim 0.32\% X_0$, thin IST $\sim 1.32\% X_0$.

Thick PXL $\sim 0.64\% X_0$, thick IST $\sim 2.64\% X_0$.

Reconstructed D⁰ signal was scaled to match the expected D⁰ production yield \times B.R. per central Au + Au collision at 200 GeV. The distribution of background was scaled to the expected background level by taking into account the random combination, particle mis-identification, high p_T proton contamination. Due to small statistics and large fluctuation of the Hijing background at high p_T , we used exponential function to extrapolate the background shape to high p_T . Different cuts

were used for the different background suppression. The difference of the background shape by varying the cuts was taken into account as background systematical uncertainty.

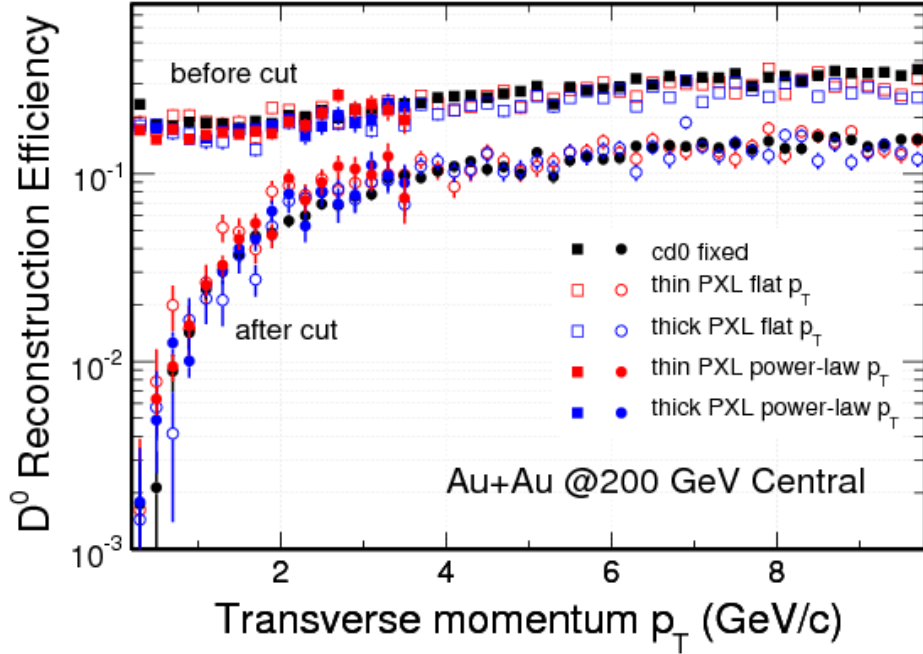


Figure 1: D^0 reconstruction efficiencies in different geometry and different input p_T distributions. TOF PID was used for these efficiencies except “cd0 fixed”.

The significance was obtained in each p_T bin. Figure 2 shows the significance distributions for thin PXL with flat p_T (black circles), thick PXL with flat p_T (red squares), thin PXL with power-law p_T (green reversed triangles) and thick PXL with power-law p_T (blue triangles). The significance of D^0 reconstruction with thick PXL geometry is lower than that with thin PXL geometry, but there is no much difference at high p_T (>3 GeV/c). The power-law p_T distribution was used to more realistically simulate the statistical errors at low p_T in different binning. We see clearly the capability to measure D^0 as low p_T as 0.5 GeV/c.

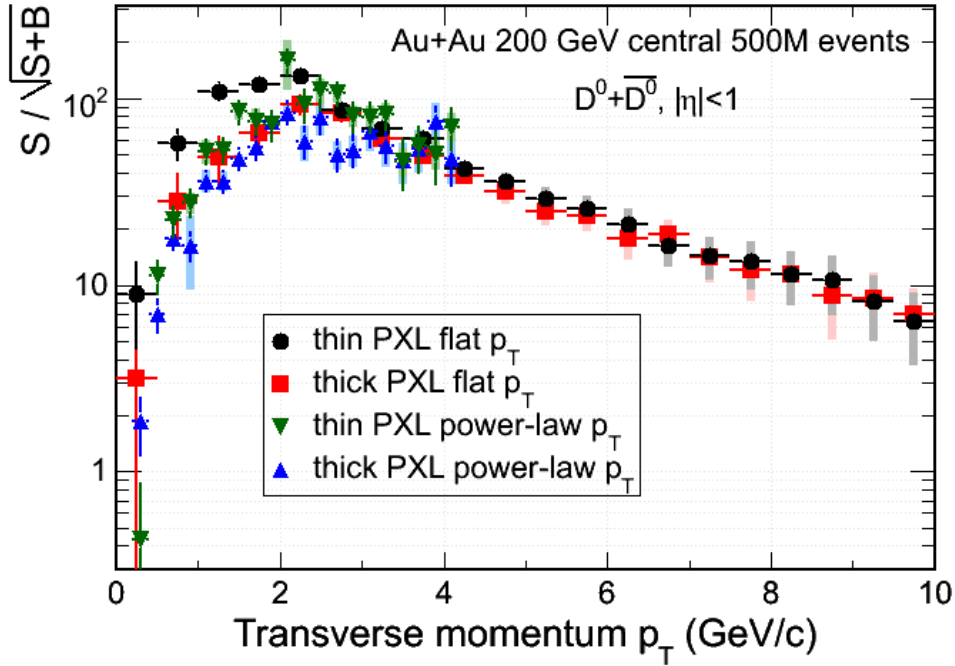


Figure 2: D^0 reconstruction significances with flat/power-law p_T distributions in thin/thick PXL geometry configurations.

===== Charm v_2 and R_{CP} texts are already in HFT_CDR_v10.pdf =====

===== The main changes compared to CD0 for both v_2 and R_{CP} plots =====

The new geometry was used in PIXEL simulation. And more realistic particle identification was used. Low p_T (1-3 GeV/c) particle identification by the BTOF detector rejected most of the protons and partially separated kaons and pions. The good PID capability suppressed the random combinatorial background. At high p_T (>3 GeV/c), only part of the proton was rejected, the upper limit (lose cut on m^2 distribution) of the proton contamination was taken into account in the background. Add one more data point (narrower binning) at low p_T for $D^0 v_2$ (Figure 3).

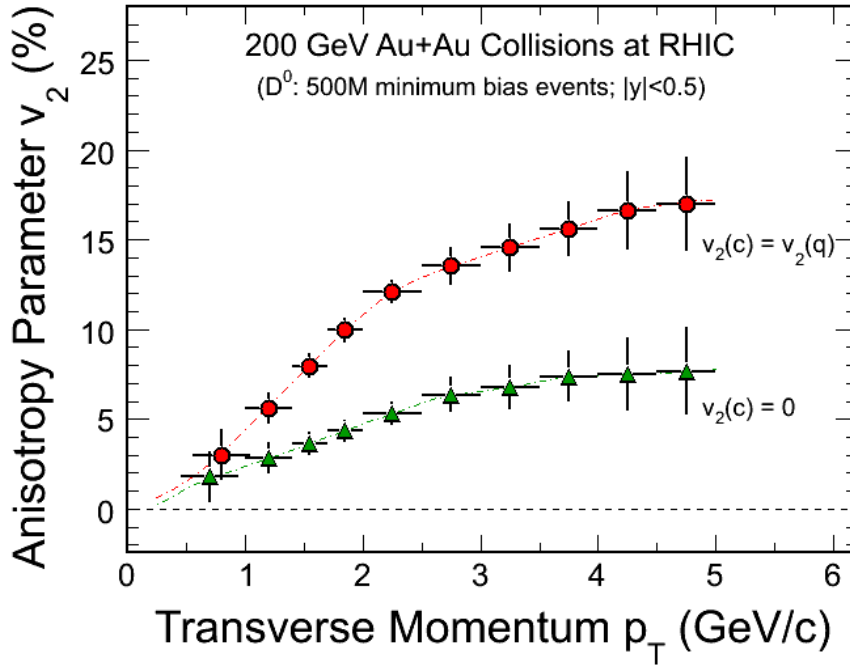


Figure 3: v_2 as a function of p_T for the case of charm flow the same as light quark flow (red) and for the case where charm does not flow (green). The statistical errors as a function of p_T are estimated for 500 M 200 GeV Au+Au minimum bias events.

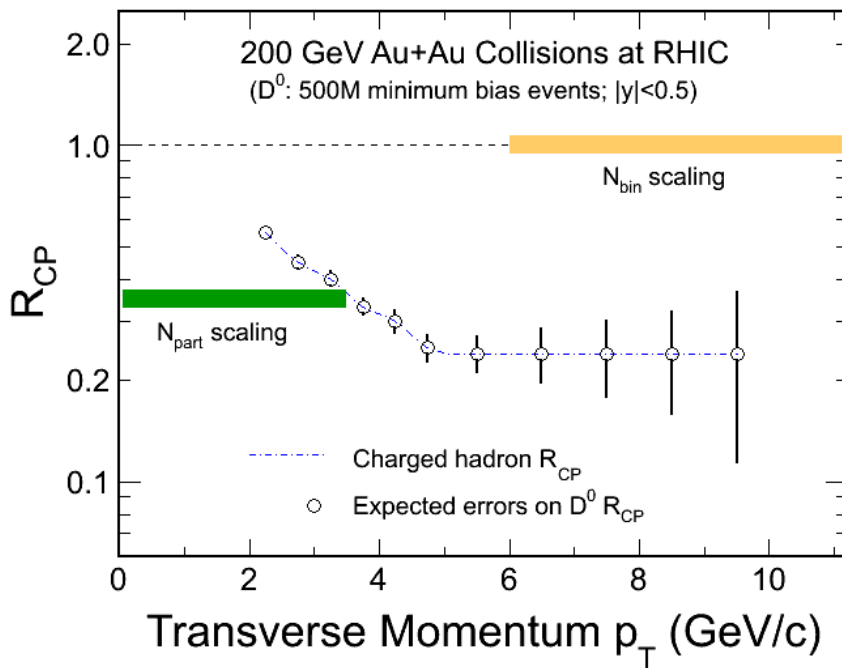


Figure 4: Assuming $D^0 R_{CP}$ follows charged hadron R_{CP} . Expected errors for a R_{CP} measurement as a function of p_T are estimated for 500 M 200 GeV Au+Au minimum bias events.